Heterogeneous Distribution of Entanglements in the Polymer Melt and Its Influence on Crystallization

Dirk R. Lippits,[†,§] Sanjay Rastogi,*[,†,‡] Günther W. H. Höhne,[†] Brahim Mezari,[†] and Pieter C. M. M. Magusin[†]

Department of Chemical Engineering and Chemistry/ The Dutch Polymer Institute, Eindhoven University of Technology, P.O. Box 513; 5600MB Eindhoven, The Netherlands, IPTME, Loughborough University, Leicestershire LE11 3TU, U.K., and DSM Research, P.O. Box 18, 6160 MD, Geleen, The Netherlands

Received October 3, 2006; Revised Manuscript Received November 19, 2006

ABSTRACT: Recently we demonstrated that it is possible to obtain single chains forming single crystals, where chains are adjacently re-entrant. It is feasible to melt these crystals, either by simple consecutive detachment of chain stems from the crystalline substrate or by cluster melting, where several chain stems are involved. The consecutive detachment of chain stems occurs at the melting point predicted from the Gibbs−Thomson equation, whereas the cluster melting takes place at much higher temperatures. Melting by consecutive detachment of chain stems from the crystal substrate and their diffusion in the melt ultimately results in a new melt state having a heterogeneous distribution of physical entanglements. Because of differences in the transverse relaxation times of the chains in the entangled and disentangled domains, solid-state NMR is the technique used to follow differences in the molecular mobility of the two domains. In this paper, with the help of solid-state NMR, we follow the mechanism involved in the development of the heterogeneous melt state. Observations are that the entangled and disentangled domains are maintained at higher temperatures resulting into a thermodynamically nonequilibrium melt state. On cooling, the heterogeneous melt influence of entanglements on the initial stages of crystallization is followed. It is found that the disentangled chains segments crystallize faster than the entangled chains, which is suggestive for the homogeneous nucleation to occur faster than the heterogeneous nucleation. Rheological studies are performed to follow the influence of disentangled domains on crystallization. With the increasing number of entanglements per unit chain, the time required for the onset of crystallization increases. In the sample from the same batch having lesser number of entanglements per unit chain, the crystallization time can be reduced by a decade.

Introduction

In semicrystalline polymers crystalline regions are linked by amorphous domains. Depending on the crystallization conditions, chain stiffness, and molecular weight, a chain may traverse between crystals or fold back within the parent crystal. In this paper, we investigate a well studied flexible polymer—an ultrahigh molecular weight linear polyethylene of molar mass greater than 10^6 g/mol (UHMW−PE). Entanglements present in the amorphous phase influence mechanical deformation of the polymer in the solid state, which show a strong dependence on the synthesis conditions.[1−3]

Entanglements in the amorphous region can be also controlled by crystallizing the polymer from solution. Below a critical initial concentration, the entanglements within the amorphous phase of the resulting material are reduced to such an extent that the solution cast films can be drawn for more than 150 times in the solid state.[4] Recently, we demonstrated that careful synthesis with a single site catalyst produces PE with a single chain forming a single crystal. These crystals can be drawn in the solid state more than 150 times.[3] The solid-state drawability is lost once the materials are molten and crystallized subsequently. This loss in drawability is attributed to the formation of entanglements in the amorphous region of the semicrystalline polymer, influencing the chain topology between the crystalline domains. Synthesis with the highly active heterogeneous Ziegler−Natta catalyst yields nascent (entangled) UHMW−PE, which is less drawable in the solid state (7 times), indicating the influence of the synthesis conditions on the topological chain structure in the amorphous region of the semicrystalline polymers.

The experimental observations are that the melting temperatures of the solution, nascent (i.e., directly obtained from synthesis), and melt-crystallized samples of the same polymer are distinctly different. For example, on heating at 10 °C/min, nascent UHMW−PE melts around 141 °C, close to the reported equilibrium melting temperature for polyethylene of 141.5 °C. Such high melting temperature has been a subject of debate. Using electron microscopy and DSC, Engelen[5] et al. conclusively showed that the nascent crystals are folded chain crystals. Thus, the high melting temperature was attributed to fast reorganization leading to successive thickening prior to melting. However, no experimental evidence of successive thickening was provided. On the contrary Kurelec et al. showed that even on annealing close to the melting point for several hours these nascent crystals do not exceed a value of 26 nm.[6,7] The melting temperature predicted from the Gibbs−Thomson equation for polyethylene[8] [$T_m = 414.2 - 259.7/l$] for a lamellae thickness of 26 nm is 131 °C.[9] Furthermore, the high melting temperature of 141 °C is lost on the second heating, where a melting temperature of 135 °C[5] is measured. A similar discrepancy is observed between the first and second heating run of solution crystallized UHMW−PE, where the lamellae double their initial thickness upon annealing below the melting temperature to a

* Corresponding author. E-mail: s.rastogi@tue.nl; s.rastogi@lboro.ac.uk.
† Department of Chemical Engineering and Chemistry/The Dutch Polymer Institute, Eindhoven University of Technology.
‡ IPTME, Loughborough University.
§ DSM Research.

10.1021/ma0622837 CCC: $37.00
Published on Web 01/19/2007

maximum of 25 nm.[10] The melting temperature predicted from the Gibbs−Thomson equation for a lamellae thickness of 25 nm is also approximately 131 °C, 5 °C lower than the experimentally observed melting point of 136 °C. Furthermore, the high melting temperature of 136 °C is lost on the second heating, where a melting temperature of 131 °C is measured.

The melting aspects involved in nascent, melt-crystallized, and solution-crystallized polymers cannot be explained by existing thermodynamic concepts alone. In a recent publication, we correlated the time and temperature required for melting to the chain topology in the amorphous phase.[11] To recall, depending on the temperature, it is feasible to melt crystals having disentangled amorphous regions by simple consecutive detachment of chain stems from the crystalline substrate (region II in Figure 1a) or by cluster melting where several chain stems are involved (region I in Figure 1a). The temperature at which melting occurs via consecutive detachment of chain stems satisfy the Gibbs−Thomson equation, whereas the cluster melting involving several chain stems occurs at a much higher temperature for the predicted crystal thickness.

The two different mechanisms involved in the crystal melting have implications on the melt state.[3] For example, melting by the consecutive detachment of chain stems from the crystal substrate and their diffusion in the melt ultimately result in a new melt state, having a heterogeneous distribution of physical entanglements. (Figure 1b, described by slow melting). With combined DSC, rheology, and solid-state NMR studies it is shown that the disentangled domains present next to the entangled domains possess higher local mobility than the entangled domains, ultimately causing a lower elastic modulus. The fraction of the entangled and disentangled domains is maintained at higher temperatures, leading to a thermodynamically nonequilibrium melt state. A theoretical explanation for the long-living character of the melt state is given in ref 12. On the contrary, in cluster melting where several chain stems (initially disentangled) can simultaneously adopt the random coil, entanglements that are formed get homogeneously distributed in the melt (Figure 1b, described by fast melting).

In this paper we aim to probe the mechanism involved in melting of the single chain forming single crystals by solid-state NMR. On melting via consecutive detachment of chain stems, the resultant heterogeneous melt, having differences in local chain mobility, which arises from differences in the distribution of chain entanglements within a chain's contour, provides a unique opportunity to investigate the influence of entanglements on crystallization aspects. From solid-state NMR, it is feasible to make a distinction in the local mobility of the disentangled and entangled domains. Crystallization, which is a nucleation and growth process, when probed by solid-state NMR will provide information on the differences in the crystallization kinetics of the disentangled and entangled domains. On cluster melting of the single chain forming single crystals, the elastic modulus probed by the rheometry increases in time with the entanglements formation. This provides samples (from the same synthesis batch) where the number of entanglements can be varied. By use of these series of samples, the influence of entanglements on polymer crystallization will be investigated.

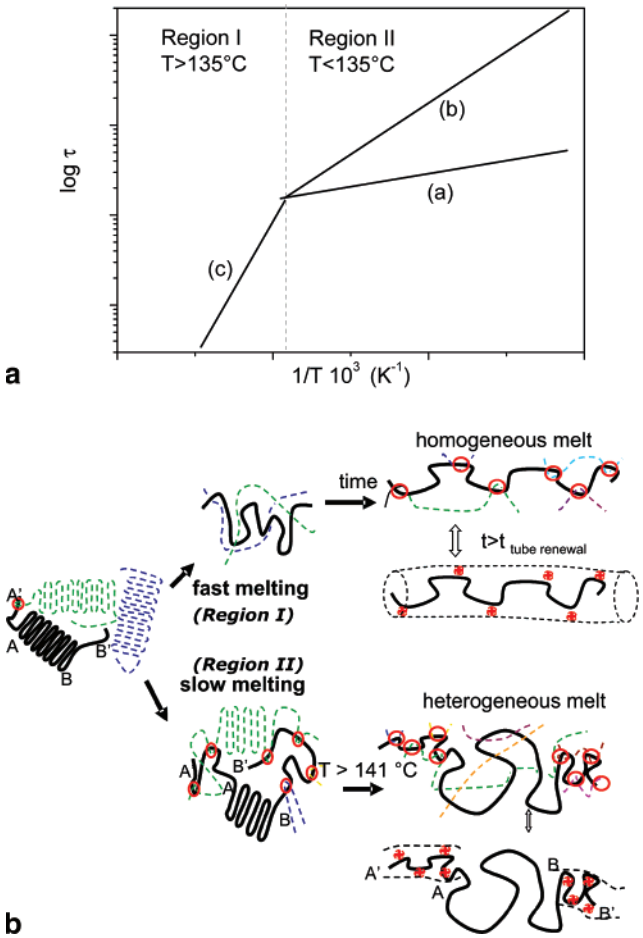

Figure 1. (a) Arrhenius plot of the melting of the nascent disentangled UHMW−PE. The activation energies of the involved processes follow from the different slopes of the data-curves. Reproduced with permission from ref 11. Copyright 2006 American Physical Society. In the region II, below 135 °C, the crystals can be melted by consecutive detachment of single (slope a) or a few (slope b) chain stems from the crystal surface. In the region I, above 135 °C, crystals are melted by random clusters, where several chain stems are involved (b) Melting process of the disentangled nascent crystals during fast or slow heating. Reproduced with permission from ref 3. Copyright 2005 Nature Publishing Group. Upon fast heating (region I of Figure 1a) the chains are likely to get mixed, leading to a gradual increase in the storage modulus with the formation of entanglements, ultimately resulting into a homogeneous distribution of the entanglements in the melt. On annealing below 135 °C, with the consecutive detachment of chain stems from the crystal substrate and their diffusion in the melt, a normal entangled amorphous phase is formed. On heating above 135 °C, the remainder of the crystal melts creating a mobile amorphous phase. The two amorphous phases, mobile and normal, do not mix even above the melting temperature. This leads to the origin of a melt having differences in the local mobility of the two amorphous components. Entanglements are encircled.

Experimental Section

Materials. To correlate the melting behavior of UHMW−PE to the chain topology, two different samples are used. The nascent grades differ in synthesis conditions and catalyst type. The nascent entangled sample is a commercial grade of Montell (1900CM) synthesized with a heterogeneous Ziegler−Natta catalyst, having molar mass of 4.5×10^6 g/mol, polydispersity 8. The nascent disentangled grade is synthesized at temperatures below the dissolution temperature using a homogeneous metallocene catalyst, having molar mass of 3.6×10^6 g/mol, polydispersity 3. The samples used for the present studies are the same as those used for the previous studies.[3,11]

Experimental Techniques. Rheometry. Oscillatory shear measurements in the linear visco-elastic region are performed using an Advanced Rheometrics Expansion System (ARES). Measurements are carried out using the parallel plate geometry (8 mm diameter) in nitrogen atmosphere. The elastic modulus is followed as a function of time at a constant frequency of 10 rad/s, and at a constant strain of 0.5%. To follow the melting, the samples were kept at constant temperature of 134 °C below the peak melting point of 141 °C. Before measurements the samples are heated with

1 °C/min from 120 °C to 134 °C. The pre-melting of the polymer is used to achieve a good adhesion between the sample and the plates. To monitor any slippage between the plates and the polymer, an oscilloscope is attached to follow any changes in the applied strain. To follow the crystallization kinetics, the samples were cooled from the melt with 1 °C/min to the desired temperature. During the measurement the temperature is kept constant

Solid State ^{1}H NMR. NMR experiments are carried out without sample rotation on a Bruker DMX spectrometer operating at a ^{1}H NMR frequency of 500 MHz and equipped with a special (7 mm MAS) probe head that resists temperatures above 150 °C. The transverse relaxation time T_2 is measured using a two pulse sequence $90°-\tau-180°-\tau-$aq with a variable τ time starting from $\tau = 2$ μs. The 90° pulse length was 5 μs and the repetition time was 3 s, which proved long enough for quantitative measurements. The relaxation decay is characterized by 60 data points at properly selected echo times. This pulse sequence is chosen because it offers the possibility to both qualitatively as well as quantitatively analyze relaxation of the amorphous and crystalline components. Temperature calibration is carried out by monitoring peak separation in the ^{1}H NMR spectrum of glycol and the melting-induced ^{1}H NMR line-narrowing of a series of compounds also employed as DSC reference materials. ^{1}H NMR spin−spin relaxation decays are obtained from the total integral of the spectra after Fourier transformation, phase- and baseline correction. The relaxation decay is analyzed by a nonlinear least-square fitting. The relaxation times are determined by fitting the relaxation data with a sum of two or three exponentials. From the determined relaxation times below the melting point appropriate τ-delay times are chosen for real-time monitoring of the T_2 relaxation by 12 data points. In this way it is possible to follow the changes in the sample with 5 min intervals.

Results and Discussions

Melting in UHMW—PE Probed by Solid-State NMR. Polymer ^{1}H NMR line shapes and spin−spin (T_2) relaxation are strongly affected by rotational chain motions at time scales $<10^{-3}$ s. The more restricted the motion, the broader is the resonance and the faster the relaxation decay of the so-called Hahn-echo produced by a $90°-\tau-180°-\tau$ pulse sequence vs the echo time 2τ. Spin−spin relaxation is a better measure for polymer chain motion than the line shape, because the latter is also broadened by other mechanisms, which are eliminated in the Hahn-echo experiment. ^{1}H NMR T_2 relaxometry is therefore a regular tool to determine entanglement- and cross-link density in rubbers[13−16] and polymers melts.[17,18]At $T >> T_g$ chain mobility at time scales $<10^{-3}$ s is controlled by chemical cross-link's and physical entanglements with lifetimes $>10^{-3}$ s. The underlying assumption is that polymer motions are divided into fast and slow polymer motions at the 10^{-3} s time scale without significant intermediate fraction. To distinguish between the crystalline and amorphous phases of nascent entangled and nascent disentangled UHMW−PE, the relatively robust and quantitative Hahn-echo method as a tool is applied.

^{1}H NMR Hahn echo decays are monitored at a constant temperature (Figure 2 and Figure 3). Between the experiments at different temperatures, the sample is heated at a rate of 0.1 °C/min. Below the onset of melting temperature, the observed Hahn-echo decays of the nascent entangled UHMW−PE sample are well described in terms of two exponential components (Figure 2). The fastest component has a fairly temperature-independent short T_2 value ~10 μs and disappears above 140 °C. This fast relaxation time is assigned to the rigid, crystalline phase. Above 120 °C, the long T_2 relaxation time of the amorphous fraction increases strongly with temperature. The steepest increase occurs around the melting point T_m ~140 °C. Apparently, below T_m chain motion in the entangled amorphous phase is confined by the crystalline domains. The resulting melt state is described by a single T_2 relaxation time of ~1 ms. This value of 1 ms is equal to the generally observed T_2 value for polyethylene with molecular masses greater than 2×10^5 g/mol.[19,20]

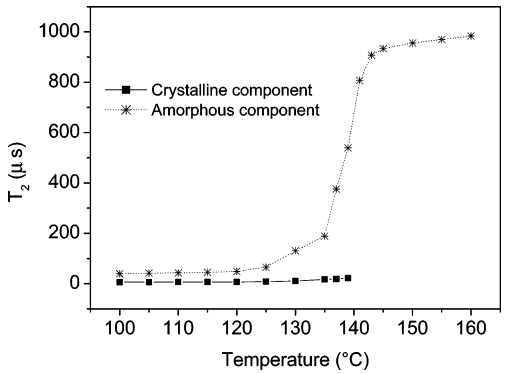

Figure 2. T_2 relaxation time vs temperature of nascent entangled UHMW−PE. The T_2 relaxation time is determined using curve fitting the ^{1}H NMR Hahn echo decays.

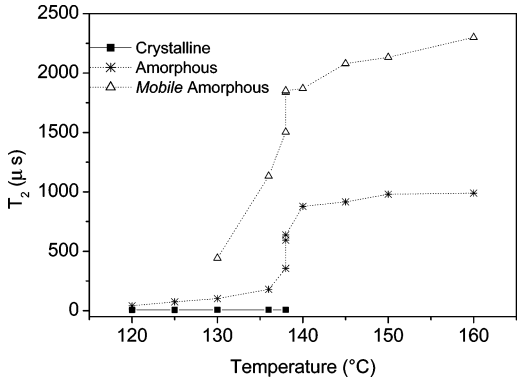

Figure 3. T_2 relaxation time vs temperature of the nascent disentangled UHMW−PE. The T_2 relaxation time is determined using curve fitting the ^{1}H NMR Hahn echo decays.

Using similar heating protocol a third T_2 component seems to show up in the Hahn-echo decays of the nascent disentangled sample (Figure 3). This component appears in addition to the crystalline and amorphous T_2 components also found for the nascent entangled UHMW−PE. The short T_2 attributed to the crystalline phase and the long T_2 attributed to the amorphous phase of the disentangled nascent sample are similar to the T_2 relaxation times determined for the crystalline and the amorphous phases of the nascent entangled sample. The value of this third T_2 component is about 2−3 times longer than that of the amorphous phase. Because of its long T_2 value, we attribute the third T_2 component to a more *mobile* type of amorphous phase to be distinguished from the *normal* amorphous phase observed for the entangled and nascent disentangled UHMW−PE.

Quantitative determination of the nascent disentangled sample is shown in Figure 4. The crystalline fraction (shortest T_2 component) of approximately 72% determined from the Hahn-echo decay at 120 °C is consistent with the crystallinity of the sample estimated from DSC. As the crystallinity decreases with increasing temperature from 130 to 137 °C, the *normal* amorphous fraction increases (Figure 4). When the temperature is increased further above 137 °C, with the disappearance of the crystalline phase, a simultaneous increase in the more *mobile* amorphous phase occurs.

To recall, melting at the low temperatures (with 0.1 °C/min from 130 to 137 °C, region II in Figure 1a) is associated with

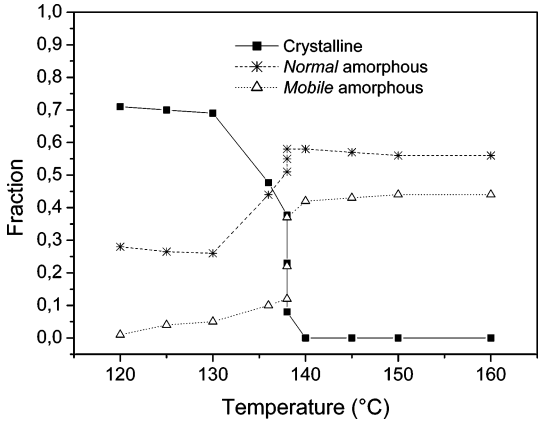

Figure 4. Quantitative changes in the relative fractions of the crystalline, mobile amorphous and normal amorphous components of the nascent disentangled UHMW−PE sample with temperature as probed from the hahn echo pulse program.

the successive detachment and diffusion of a few crystal stems from the crystal surface (Figure 1b described for slow melting). The increase of the normal amorphous fraction suggests that the polymer chain stems that are molten by the successive detachment are able to entangle with the surrounding amorphous phase. When the temperature is increased further with the melting of the remainder of the disentangled crystalline fraction (approximately 40%) a highly *mobile* amorphous component, *of the same fraction*, evolves. The amount of the highly *mobile* amorphous fraction as well as the *normal* amorphous fraction remains almost constant on increasing temperature. This suggests a barrier for the mixing of the two amorphous-phases. From the NMR studies it can be concluded that since the polyethylene chains are chemically uniform. Upon slow melting of the disentangled nascent crystals, the presence of the two amorphous fractions with two different mobilities above 140 °C will arise from the "heterogeneous" distribution of entanglements.

On *fast* heating (10 °C/min, cluster melting depicted in region I of Figure 1a and shown schematically in Figure 1b) of the nascent disentangled sample to its melt state, (see Figure 5a spin relaxation occurs much faster compared to the same disentangled sample when heated slowly to the melt. From the figure it is also evident that in contrast to the *slowly* heated sample in the *fast* heated sample the *mobile* amorphous component is absent and thus the T_2-relaxation can be described with a single relaxation time. The T_2-relaxation at 150 °C determined for the entangled nascent sample, shown in Figure 5b, is independent of heating rate. Using the different T_2-relaxation time as a filter, thereby suppressing the less-mobile fractions of the melt, we observe significant differences in the peak width of the NMR spectrum of the two melt states arising with different heating rates from the initially nascent disentangled sample. The narrower peak of the slowly heated melt indicates a higher local mobility in part of the sample. Whereas the T_2-filtered peak width of the initially entangled sample is independent of the heating rate (Figure 5b). The observed peak width is similar to the fast heated disentangled melt, Figure 5a. In fact, an increase in T_2 filter time leads to suppression of the rigid fractions of the sample and decreasing peak width in the slow heated disentangled melts, strengthening the idea of heterogeneity in the local mobility.

These dynamic NMR results suggest that upon fast melting, associated with melting in clusters of 7−8 polymer chain stems, the chains are homogenously distributed in the melt, resulting in a homogeneous distribution of entanglements. If the nascent

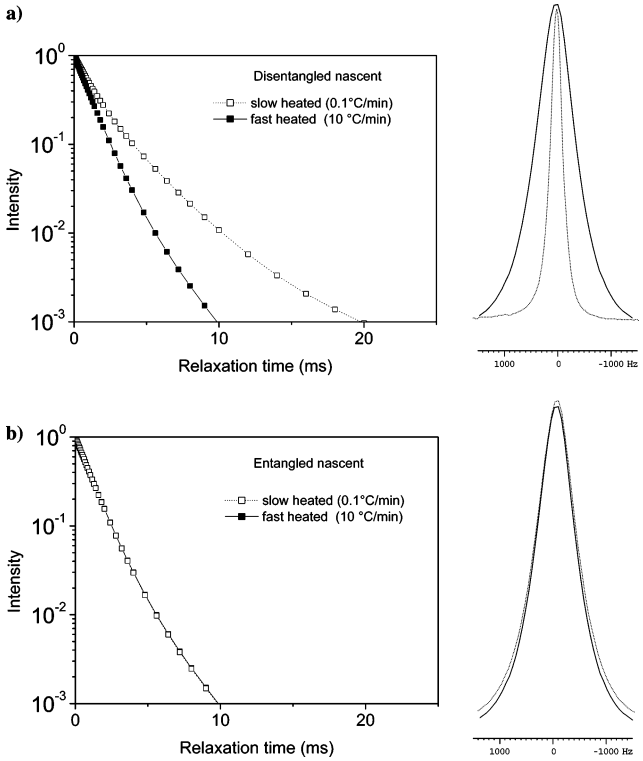

Figure 5. NMR line shapes and T_2 relaxation curves of fast (10 °C/min, filled squares) and slow (0.1 °C/min, unfilled square) heated UHMW−PE melts of the initially entangled and disentangled nascent samples. Experiments are performed at 150 °C. Melts of the entangled grade do not show any heating rate dependence in their T_2 relaxation behavior, whereas significant slower T_2 relaxation is observed for the slow heated nascent disentangled melt, indicating a higher local molecular mobility for fractions of the melt. The dynamic heterogeneity of the slow heated disentangled nascent sample can be monitored as well via variation of the line width in the T_2-filtered spectra. (10 ms is the applied T_2 relaxation filter time.) It can be seen that the slowly heated nascent disentangled sample show a sharp peak compared fast heated sample. The nascent entangled grade does not show a difference between fast and slow heating.

disentangled UHMW−PE sample is given more time to melt (slow heating, region II in Figure 1a), the crystals are molten first from the sides (chain ends, slow melting depicted in Figure 1b) before the complete breakdown of the crystal lattice occurs. The resulting melt state contains a heterogeneous distribution of chain entanglements. The heterogeneous melt state exhibits interesting rheological phenomena as summarized in ref 3 and also summarized later in this manuscript.

Melt Mechanism. To attribute the structural changes on melting as depicted by the solid-state NMR, here we recall that melting depicted by DSC[11] in region II of Figure 1a occurs via detachment of single chain stems on the side surface of a crystal. When the results from DSC and solid-state NMR are combined, the earlier proposed hypothesis[3] for the melt mechanism involved in melting of the nascent disentangled UHMW−PE can be further strengthened. Figure 1b depicts the slow melting of the nascent disentangled crystals. The adjacently re-entrant chains melt by consecutive detachment of chain segments equal to the crystal thickness (from the crystal sides) from the crystal lattice (AA′ and BB′ in Figure 1b). The initially disentangled chains will form entanglements by reptation (circles) and will result in a T_2 relaxation time (up to 1 ms) equivalent to a normal entangled melt. When the whole crystal is melted at higher temperatures, the section AB in Figure 1b, will transform from a disentangled crystal to a disentangled amorphous phase (as was shown in the NMR experiments). Because of the absence

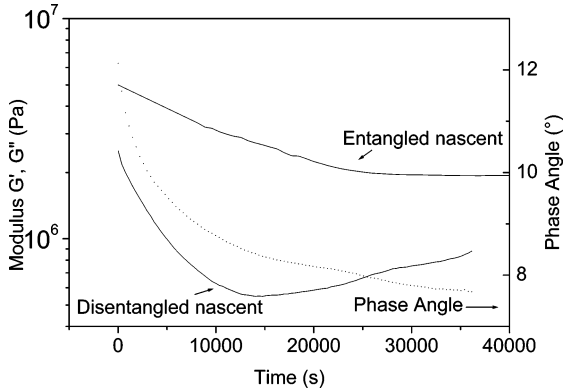

Figure 6. Elastic modulus of the entangled and disentangled nascent UHMW−PE as a function of time at a fixed frequency of 10 rad/s, strain (0.5%), and temperature 134 °C. The phase angle plotted in the figure is from the annealing experiment of the disentangled sample.

of physical entanglements, the disentangled component of the amorphous fraction can be described by a high T_2 value (up to 2.5 ms) referring to the higher local mobility. Thus, depending on the melting via consecutive detachment of chain stems (region II, Figure 1a) or cluster melting (region I, Figure 1a), chain dynamics in the resultant melt state of the nascent disentangled crystals can be altered. Detailed study on the influence of heating rate on chain dynamics is reported elsewhere.[3]

Contrary to the slow melting, a complete collapse of the crystal lattice occurs upon fast melting. This causes an instant free movement of the chain ends in the melt, ultimately forming homogeneous distribution of entanglements (Figure 1b).

In the nascent entangled samples, physical entanglements present in the amorphous phase of the semicrystalline polymer restrict the consecutive detachment of chains. Therefore, the low activation energy component (a) in Figure 1a is absent. Thus, on melting, independent of the heating rate, entanglements present in the amorphous phase get homogeneously distributed along the main chain.

Differences in the melting process of the entangled and disentangled nascent polymers can be also be probed by rheometry. The melting process can be followed by keeping the entangled and disentangled samples at a constant annealing temperature of 134 °C. The elastic modulus is followed as a function of time at a constant strain of 0.5% (inside the viscoelastic linear regime) and frequency of 10 rad/s (inside the rubbery plateau modulus time frame). When the disentangled and entangled nascent samples are annealed, the phase angle decreases with time, Figure 6. This decrease in phase angle and the modulus is attributed to melting of the crystals. Distinction between the modulus of the entangled and disentangled polymers is evident. When the nascent entangled sample melts, the elastic modulus decreases to 2 MPa, corresponding to the plateau modulus of the fully entangled melt state, whereas the disentangled sample shows an initial drop in the modulus to 0.6 MPa followed by an increase with time. These rheological differences originating from the melting behavior of the nascent entangled and nascent disentangled UHMW−PE are in agreement with the differences observed on crystal melting by solid-state NMR. We recall that as the entangled nascent sample melts, a *normal* melt state arises, which is entangled. Whereas on slow melting of the disentangled nascent sample, a *mobile* melt state together with a normal melt state is realized. The presence of this mobile melt state causes a lower plateau modulus than that anticipated from the normal melt state. Hence we can designate the origin of the *mobile* component in the melt to be disentangled. In Figure 6, the increase in plateau modulus of the disentangled nascent polymer after 15000 s is due to the increasing number of entanglements.

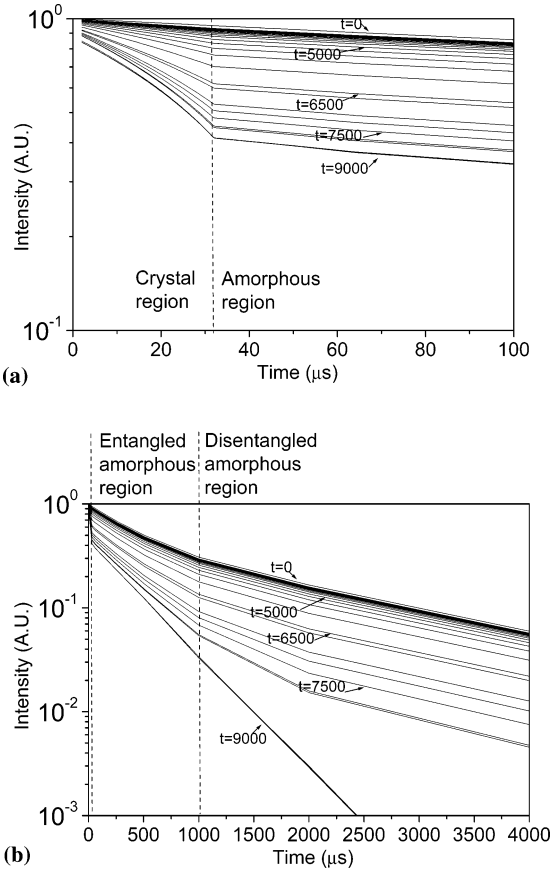

Figure 7. T_2 decay curve obtained using a Hahn-echo pulse program during isothermal crystallization at 127 °C. The sample was cooled from the heterogeneous melt state at 160 to 127 °C with 1 °C/min. In the figure, two distinct slopes can be seen, a steep slope from 0 to 32 μs (a), related to the crystalline phase, and 32−4000 μs related to the amorphous phases. A closer look of the T_2 − relaxation in the amorphous phase (b) shows the presence of two slopes in the region $t = 0$ to $t = 6500$ s. The two slopes arise from the differences in the mobility of the disentangled and entangled amorphous phases.

Role of Chain Entanglements in Crystallization: Homogeneous vs Heterogeneous Nucleation. The heterogeneous melt state obtained on slow melting, constitutes entangled and disentangled domains, providing an opportunity to investigate the influence of entanglements on polymer crystallization—in particular, the nucleation process, which has been a subject of dispute. It has been often debated that nucleation occurs via chain disentanglement from the entangled melt or via clustering of the disentangled domains pushing the entanglements within the amorphous region.[22] As stated earlier solid-state NMR is an experimental tool capable of making a distinction in the local mobilities of the disentangled and entangled domains. Differences in the local mobility are apparent from the two different relaxation times for the two amorphous domains, as shown in Figure 3. Thus, by following the crystallization aspects of the two domains at a fixed temperature, it can be feasible to probe the nucleation process at the molecular length scale.

Figure 7 shows the T_2 relaxation of the heterogeneous melt during crystallization at 127 °C, recorded at an interval of 5 min. Compared to the amorphous phases having the T_2 relaxation times in the order of 1 ms, the T_2 relaxation time for the crystal phase is 2 decades faster, in the order of microseconds. Consequence to the two very different relaxation times,

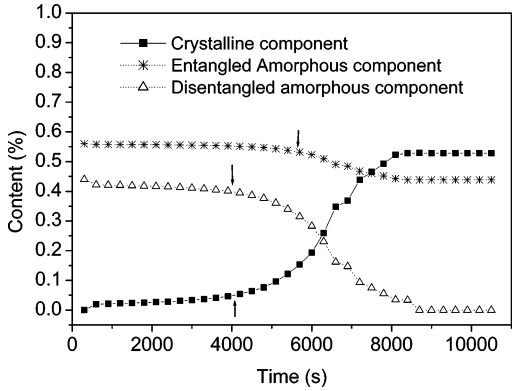

Figure 8. Quantitative determination of the three components (crystalline, entangled and disentangled amorphous), during isothermal crystallization at 127 °C. The quantitative determination is obtained by curve fitting the T_2-relaxtion curve presented in Figure 7.

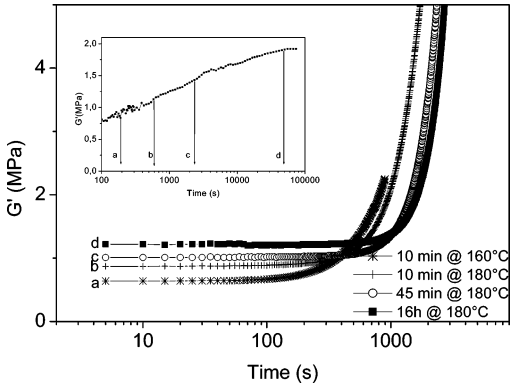

Figure 9. Buildup of complex modulus with time during isothermal crystallization is recorded at 125 °C and 10 rad/s. Samples of the nascent disentangled UHMW−PE were fast molten and left in the melt for (a) 1, (b) 10, (c) 45, and (d) 100 min. The onset in modulus refers to the onset in crystallization. The inset shows the buildup of plateau modulus of the fast molten sample at 180 °C with time. Points a, b, c, and d in the inset refer to different plateau modulus obtained on leaving the samples for different times.

the T_2 relaxation curve shows two distinct slopes as is evident from Figure 7a. The slope in the region of echo times of 0−32 μs is attributed to the crystal phase and the slope in the region greater than 32 μs to the two amorphous phases. The large differences in T_2-relaxation times of the crystalline and the amorphous phases facilitate quantitative determination of the crystalline fraction. This is obtained by curve fitting the T_2-relaxation data in the region of 0−100 μs. From the Figure 7b, it is to be noted that the slope of the amorphous region, from $t = 0$ s to $t = 6500$ s, does not change, while the crystalline component increases. Thus, on curve fitting the amorphous fraction in the region of 32 μs to 4 ms echo times, it is observed that the qualitatively determined T_2 relaxation times of the both amorphous phases remain nearly unchanged up to a crystallinity of approximately 45% (at $t = 6500$ s). Since the T_2-relaxation times of the two amorphous phases are almost constant, the relative fraction of the two amorphous phases can be determined by curve fitting the T_2-relaxation data in the region of 32 μs to 4 ms echo times.

Figure 8 shows changes in the fraction of the crystalline and the amorphous (entangled and disentangled) components during isothermal crystallization at 127 °C. Arrows in Figure 8 correspond to the onset of the decrease in the fraction of the two amorphous phases and the increase in the crystalline fraction. It is to be noted that the decrease in the fraction of the mobile disentangled amorphous component occurs much earlier than the entangled amorphous component. With the decrease in the fraction of the disentangled amorphous component, a simultaneous increase in the fraction of the crystalline component occurs. This is suggestive for the earlier onset of the crystallization of the disentangled amorphous component compared to the entangled amorphous component. The role of entanglements in the nucleation process becomes more evident by the rate at which the disentangled mobile fraction decreases relative to the entangled fraction—to quote for the given time while the entangled amorphous component decreases by approximately 10%, the disentangled fraction of approximately 40% crystallizes completely. These studies clearly demonstrate the overriding influence of the homogeneous nucleation over the heterogeneous nucleation, provided that the chains are in the disentangled state. Homogeneous nucleation in the disentangled region followed by the crystal growth provides the possibility of crystalline disentangled domains in the solid state, likely to arise from intramolecular crystallization. The presence of disentangled crystalline domains is realized by the easy deformation of the semicrystalline polymer in the solid state, as described in Figure 6 of ref 3. Theoretical studies on intramolecular nucleation have been performed by Hu et al.[23] From their studies, the authors concluded that the intramolecular nucleation in a single homopolymer chain is independent of chain length and crystallization proceeds via homogeneous nucleation.

To investigate the influence of entanglements on crystallization, we follow the onset of crystallization with the increasing amount of entanglements using rheometry. On fast melting (region I, Figure 1) of the nascent disentangled crystals, with the formation of entanglements, as the molar mass between the entanglements decreases, the elastic modulus increases. The inset in Figure 9 depicts an increase in the storage modulus for linear polyethylene having a molar mass of 3.6×10^6 g/mol with a polydispersity of 3.0. The time required for the modulus to reach the thermodynamically equilibrium state at 180 °C is approximately 10^4 s.

Experimentally, the onset of isothermal crystallization can be monitored by measuring the dynamic modulus as a function of time at a constant strain and fixed frequency, where a strong increase in modulus indicates the onset of crystallization. Figure 9 shows that nascent disentangled crystals, heated fast to 180 °C and left for 1 min before being cooled to an isothermal crystallization temperature of 125 °C, show an onset in the buildup of modulus after approximately 250 s (curve *a* in Figure 9). When a sample of the same grade is heated to 180 °C and left in melt at 180 °C for 10 (curve *b*), 45 (curve *c*), and 100 (curve *d*) min, respectively, the onset of the modulus increase shifts to longer times. Differences in the onset of crystallization time can be as large as an order of magnitude. The shift in plateau modulus to higher values on going from curve *a* to *d* show an increase in the number of entanglements per chain with increasing residence time of the sample in melt. From here it is concluded that with the increasing number of entanglements per chain the time required for the onset of crystallization increases.

As the disentangled nascent crystals in the region II of Figure 1a melt, a heterogeneous melt is evolved having disentangled and entangled domains. To recall, NMR studies performed on the heterogeneous melt show crystallization of the disentangled domains much earlier than the entangled domains. To further investigate the influence of disentangled regions in crystallization of the polymer a rheological study on the heterogeneous melt is performed. Figure 10 shows the influence on crystallization of the heterogeneous and homogeneous entangled melt

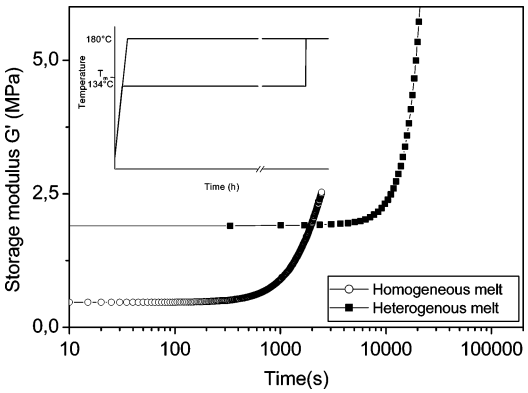

Figure 10. . Comparison in the isothermal crystallization behavior recorded at 127 °C and 10 rad/s of the two different melt states, homogeneous and heterogeneous. The inset shows the two different routes to obtain the two different melt states in the same polymer, nascent disentangled UHMW−PE.

states with a different number of entanglements per unit chain. To obtain the homogeneous entangled melt state the disentangled nascent crystals are heated fast to 180 °C, left at 180 °C for 100 min, and, subsequently, cooled to the isothermal crystallization temperature of (in this case) 127 °C. Whereas the sample having a heterogeneous distribution of entanglements was left at 136 °C for 18 h prior to fast heating to 180 °C. This sample was left at 180 °C for 15 min before being cooled to 127 °C. In the heterogeneous sample, the onset of the storage modulus occurs a decade earlier than the homogeneously entangled melt. This shows faster crystallization of the heterogeneous melt state having a larger molar mass between entanglements as compared to the homogeneous entangled melt state.

Successive crystallization and melting of the heterogeneous melt state ultimately results in the homogeneous distribution of entanglements, as shown in ref 3. This process can be well understood by considering the rate of gain in entropy on melting. These findings invoke the heating rate dependence on the buildup of modulus, the subject of a following publication.

Conclusions

When the earlier stages of crystallization of the melt having the disentangled and the entangled domains is followed, solid-state NMR shows an earlier onset of crystallization of the chains residing in the disentangled domains compared to the entangled domains—indicative of the faster intramolecular homogeneous nucleation compared to the normally anticipated heterogeneous nucleation. Rheological studies performed on the heterogeneous melt show a decade earlier onset of crystallization compared to the melt having the homogeneous distribution of entanglements. Nascent disentangled crystals provide an opportunity to follow the entanglement formation with the buildup of the elastic modulus with time. Using a series of these samples, it is shown that with the increasing number of entanglements the onset of crystallization shifts to longer times for a crystallization temperature.

Acknowledgment. The authors wish to acknowledge constructive discussions with Prof. Hans W. Spiess and Dr. Robert Graf of the Max Planck Institute for Polymers in Mainz, Germany.

References and Notes

(1) Smith, P.; Chanzy, H. D.; Rotzinger, B. P. *Polym. Commun.* **1985**, *26*, 258.
(2) Rotzinger, B. P.; Chanzy, H. D.; Smith, P. *Polymer* **1989**, *30*, 1814.
(3) Rastogi, S.; Lippits, D. R.; Peters, G. W. M.; Graf, R.; Yao, Y.; Spiess, H. W. *Nature Mat.* **2005**, *4*, 635.
(4) Lemstra, P. J.; Bastiaansen, C. W. M.; Rastogi, S. In *Structure Formation in Polymeric Fibers*; Salem, D. R., Ed.; Hanser: Munich, Germany, 2000; Chapter 5; ISBN 1-56990-306-9.
(5) Tervoort-Engelen, Y. M. T.; Lemstra, P. J. *Polym. Commun.* **1991**, *32*, 343.
(6) Rastogi, S.; Kurelec, L.; Lippits, D.; Cuijpers, J.; Wimmer, M.;. Lemstra, P. J. *Biomacromolecules* **2005**, *6*, 942.
(7) Corbeij-Kurelec, L. Chain mobility in polymer systems. Ph.D. Thesis, Eindhoven University of Technology, 2001; Chapter 3; ISBN 90-386-3032-8. http://alexandria.tue.nl/extra2/200113706.pdf.
(8) Wunderlich, B.; Czornyj, G. *Macromolecules* **1977**, *10*, 906.
(9) The authors are aware that depending on the experimental methods used, different numerical Gibbs-Thomson equations exist; see: Cho T. Y.; Heck, B.; Strobl, G.; *Colloid Polym. Sci.* **2004**, *282*, 825. A difference arises because of different surface free energy values resulting in a somewhat different melting temperature of 136 °C for a crystal thickness of 25 nm. However, such discrepancies in the calculated melting temperatures have no implications on our experimental findings.
(10) Rastogi, S.; Spoelstra, A. B.; Goossens, J. G. P.; Lemstra, P. J. *Macromolecules* **1997**, *30*, 7880.
(11) Lippits, D. R.; Rastogi, S.; Höhne, G. W. M. *Phys. Rev. Lett.* **2006**, *96*, 218303.
(12) McLeish, T. C. B. *Soft Matter* **2007**, DOI: 10.1039/b611620e.
(13) Fry, C. G.; Lind, A. C. *Macromolecules* **1988**, *21*, 1292.
(14) Wouters, M. E. L.; Litvinov, V. M.; Binsbergen, F. L.; Goossens, J. G. P.; van Duin, M.; Dikland, H. G. *Macromolecules* **2003**, *36*, 1147.
(15) Tillier, D. L.; Meuldijk, J.; Magusin, P. C. M. M.; van Herk, A. M.; Koning, C. E. *J. Polym. A* **2005**, *43*, 3600.
(16) Orza, R. A.; Magusin, P. C. M. M.; Litvinov, V. M.; van Duin, M.; Michels, M. A. *Macromol. Symp.* **2005**, *230*, 144.
(17) Cosgrove, T.; Turner, M. J.; Griffiths, P. C.; Hollingshurst, J.; Shenton, M. J.; Semlyen, J. A. *Polymer* **1996**, *37*, 1535.
(18) Guillermo, A.; Cohen Addad, J. P.; Bytchenkoff, D. *J. Chem. Phys.* **2000**, *113*, 5098.
(19) Brereton, M. G.; Ward, I. M.; Boden, N.; Wright, P. *Macromolecules* **1991**, *24*, 2068.
(20) In monodisperse entangled polyethylene samples, we have found a molar mass independent T_2 relaxation time of approximately 1 ms. For molar masses greater than 2×10^5 g/mol, see: Lippits, D. R.; Rastogi, S.; Yao Y.; Graf, R.; Magusin, P. C. M. M. Manuscript in preparation.
(21) Yao, Y.; Graf, R.; Rastogi, S.; Spiess, H. W. Presented at IUPAC Macro 2004, Paris.
(22) Strobl, G. *Eur. Phys. J. E* **2005**, *18*, 295.
(23) Hu, W.; Frenkel, D.; Mathot, V. B. F. *Macromolecules* **2003**, *36*, 8178−8183.

MA0622837